# Plasma transport around dust agglomerates having complex shapes

Eric R. Keiter[a] and Mark J. Kushner[b]
*Department of Electrical and Computer Engineering, University of Illinois, 1406 West Green Street, Urbana, Illinois 61801*

(Received 1 December 1997; accepted for publication 27 February 1998)

Dust particles generated in low temperature plasmas as used for microelectronics fabrication are often agglomerates of smaller monodisperse particles. The transport of these agglomerates, and the subsequent contamination of surfaces, depends on the details of ion-momentum transfer (ion drag) to, and electrostatic forces on, the agglomerate. Given that the charge distribution on the surface of the agglomerate and local electric fields in the vicinity of the agglomerate depend on its shape, the subsequent forces on the agglomerate will also be a function of shape. In this article, we describe results from a simulation in which plasma transport around, and the charging of, agglomerates are investigated. We find that the charge distribution on the agglomerates is generally nonuniform, a consequence of both shadowing and charge depletion. The ion-momentum transfer cross section, calculated using a Monte Carlo simulation, also depends on the shape of the agglomerate. © *1998 American Institute of Physics.* [S0021-8979(98)04711-2]

## I. INTRODUCTION

Dust particle transport and charging in plasmas in the context of contamination free manufacturing of microelectronics has been the topic of a number of studies in the past few years.[1–4] The transport of charged dust particles in plasmas as used for materials processing is typically dominated by ion drag (momentum transfer from ions) and electrostatic forces. The former accelerates particles towards the peripheries of the reactor while the latter accelerates particles away from boundaries towards the peak in the plasma potential. Dust particle trapping can occur where these forces are in balance. Recently, investigations have been conducted on the agglomeration of dust particles in plasmas.[3] Dust particle agglomerates are typically composed of a collection of nearly monodisperse spherical particles. These agglomerates grow by accretion or addition of a single particle at a time, a process which requires that the incoming particle have sufficient kinetic energy to overcome the repulsive electrostatic forces between the monomer particle and the agglomerate. The details of this force depend upon the ratio of the lateral dimension of the dust particle agglomerate to the plasma shielding length. Particles which are large compared to the shielding length may have a portion of their charge screened from the incoming monomer particle, thereby increasing the probability of agglomeration. In general, agglomerates formed from energetic monomer particles tend to be compact and have a high fractal dimension. Agglomerates formed from low energy particles tend to be dendritic with a low fractal dimension.

The ion drag force on dust particles results from momentum transfer between the directed ion flux and the dust particle.[4] It is the most important mechanism for expelling dust particles from the plasma, or at least accelerating them to sheath edges where trapping may occur. The magnitude of the ion-drag force depends on the details of the orbital motion of the ion in the near vicinity of the dust particle and therefore will be sensitive to the details of the electric field near the particle. To the degree that, for a constant number of monomer particle constituents, the shape of the particle determines these fields, agglomerates having the same number of monomer particles but having different shapes will have different ion-drag cross sections. The propensity for wafer contamination by agglomerates will then be a function of their shape.

In this article, we discuss the results of a computational study of the plasma transport, charging and ion-momentum transfer cross sections of agglomerated dust particles having complex shapes in low temperature plasmas. The model developed for this study is a two-dimensional implicit plasma fluid simulation which self-consistently accounts for the charging of the particles. Ion momentum transfer cross sections are then determined from the resulting electric fields using a Monte Carlo (MC) simulation. We found that the distribution of negative charge on the surface of the particle is a sensitive function of the morphology of the agglomerate which, for dielectric materials, is typically not uniformly distributed. In part, the nonuniform charging is a consequence of both geometrical and electrostatic shielding effects, and the relative strength of these effects is dependent upon the initial conditions of the plasma, as well as the material characteristics of the particle. The models used in these studies are described in Sec. II followed by a discussion of our results in Sec. III. Our concluding remarks are in Sec. IV.

## II. DESCRIPTION OF THE MODEL

The plasma simulation we developed for this study is an implicit drift-diffusion model for a single positive ion, electrons and the electric potential. An implicit scheme was required due to the small spatial scale of the numerical mesh ($<1$ $\mu$m). Since the model is two-dimensional, the agglom-

[a]Electronic mail: keiter@uigela.ece.uiuc.edu
[b]Electronic mail: mjk@uiuc.edu

 

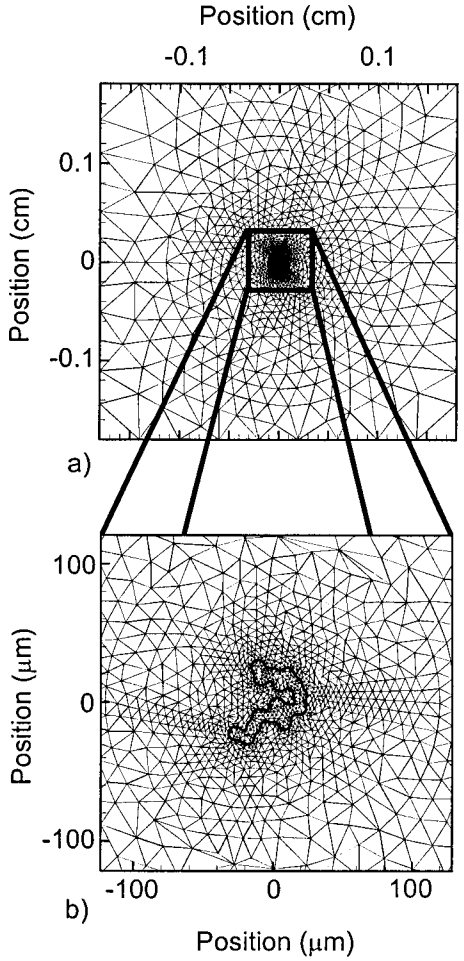


FIG. 1. A typical numerical mesh for a 16 particle agglomerate. The top figure shows the full computational domain. The lower figure shows an enlargement of the domain in the vicinity of the agglomerate.

erates can only be resolved as collections of rods, however we believe the conclusions can be generalized to three-dimensional structures. The plasma transport is being represented by a drift-diffusion formalism. Therefore, the orbital motion of ions which results in the plasma shielding distance around the particle being given by the linearized debeye length cannot be resolved.[4] As a consequence, the shielding distances which are produced by the model are most closely characterized by the electron Debeye length. Since it is the ratio of the agglomerate size to the Debeye shielding length which is the important parameter, we have chosen appropriately sized particles so that this ratio is of the desired magnitude. The calculation of the ion drag cross section, which is performed using a Monte Carlo simulation, does resolve the proper orbital motion and so the resulting cross sections should be accurate.

The plasma model uses an unstructured triangular mesh which spans approximately three orders of magnitude in resolution, from the particle dimension (submicron) to a plasma domain of 100s $\mu$m. The mesh was constructed using a commercial mesh generation program, CFD-GEOM.[5] A typical mesh for an agglomerate having 16 particles is shown in Fig. 1. We found that it was necessary that all the agglomerate surface nodes have nearest neighbor nodes inside the plasma, which accounts for the sometimes ''smooth'' appearance of multi-particle agglomerates on the mesh.

The equations solved at each mesh point in the appropriate sub-domains are

$$\frac{\partial N_i}{\partial t} = -\nabla\cdot(-D_i\nabla N_i q_i\mu_i\nabla\Phi N_i), \tag{1}$$

$$\nabla\cdot\varepsilon\ \nabla\Phi = -\sum_i\ q_i N_i - \rho, \tag{2}$$

$$\left[\frac{\partial\rho}{\partial t}\right]_s = -\nabla\cdot\sigma_s E_{||} + \sum_{\mathrm{i}}\ -\nabla\cdot(q_{\mathrm{i}}[-D_{\mathrm{i}}\nabla N_{\mathrm{i}} - q_{\mathrm{i}}\mu_{\mathrm{i}}\nabla\Phi N_{\mathrm{i}}]), \tag{3}$$

$$\left[\frac{\partial\rho}{\partial t}\right]_b = \nabla\cdot\sigma_b\nabla\Phi, \tag{4}$$

where $\Phi$ is the electric potential, $E_{\|}$ is the electric field parallel to the agglomerate surface, $N_i$ is the electron or ion density, $D_i$ is the species diffusion coefficient, $\mu_i$ is its mobility, and $\epsilon$ is the local permittivity. The term $\rho$ is the plasma charge density, $\rho_s$ is the charge density on the surface of the particle and $\rho_b$ is the charge density inside the agglomerate. The terms $\sigma_s$ and $\sigma_b$ are the surface and bulk conductivities of the agglomerate. The equations for $N$ are solved only in the plasma while Poisson's equation is solved throughout the computational domain. The equation for $\rho_s$ is solved only on the agglomerate surface nodes. The second equation for $\rho_b$ is solved throughout the interior of the dust agglomerate. We ignore changes in density due to ionization, attachment or recombination in the vicinity of the agglomerate as mean free paths for these processes are typically larger than the computational domain for the conditions of interest. The electron and ion densities are set equal and held fixed, and the electric potential is set to zero, on the outer boundaries of the computational domain.

The equations are solved implicitly through a time integration to the steady state with a dynamic time step using Newton's method within the hierarchy of the SimGen numerical software.[6] The spatial derivatives are formulated using box integration, a graphical representation of which appears in Fig. 2. The divergence operator for flux $\Gamma$ at point $j$ is

$$(\nabla\cdot\Gamma)_j = \sum_i\ \Gamma_{ij}\frac{A_{ij}}{V_j}, \tag{5}$$

where the summation is over the nearest neighbors to $j$, $\Gamma_{ij}$ is the flux between $i$ and $j$, $A_{ij}$ is the area of the face forming the perpendicular bisector between $i$ and $j$, and $V_i$ is the volume of the cell defined by the intersection of the perpendicular bisectors.

The fluxes, $\Gamma$, for each charged species will range from being diffusion dominated near the edge of the numerical domain to being drift dominated closer to the agglomerate. As a result care must be taken in choosing the discrete form of the flux, as the use of a standard central difference scheme can lead to nonphysical oscillations in the sheath region. To avoid this problem we use the discretization formulated by Scharfetter and Gummel.[7,8] In the limit of a large electric

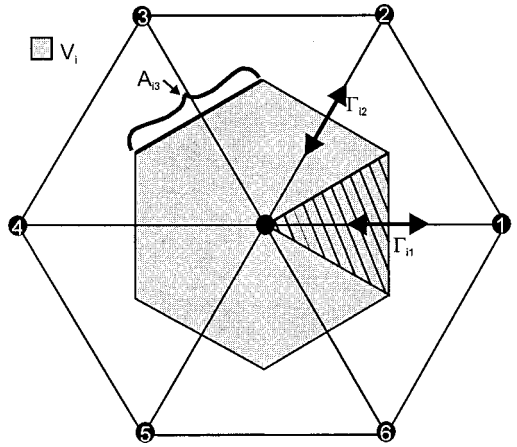


FIG. 2. Graphical representation of box integration. The volume, $V$, is for the entire shaded region. Fluxes between mesh points are computed for each ''sector'' (shown cross hatched).

field this discretization resembles an upwind difference, while in the limit of zero electric field it resembles a central difference. As the variable quantities in Eqs. (1)–(4) have values of widely varying magnitudes, we have employed the scaling scheme described in Selberherr[7] to reduce roundoff error in the solution of the matrix required in each Newton iteration.

The ion-drag momentum transfer cross section was calculated using a Monte Carlo (MC) simulation after obtaining the electric field around the agglomerate from the plasma simulation. For the purposes of the MC calculation, the two-dimensional (2D) potential from the fluid simulation was assumed to be azimuthally symmetric in three dimensions (3D) around the axis of the angle of approach. MC particles, representing ions, were launched towards the particle and their equation of motions integrated using electric fields interpolated from the unstructured mesh. The starting locations of the MC particles were varied in two ways. First, to account for the asymmetric shape of the agglomerate, the azimuthal angle of the initial trajectory (with respect to the internal axis of the agglomerate) was randomly chosen. Second, given this angle, a series of MC particles were launched with a preselected sequence of impact parameters. The spacings of the impact parameters were decreased as the agglomerate was approached in order to adequately resolve the asymmetric electric fields. The variations of angle and impact parameter are illustrated in Fig. 3. The ion-drag cross section was then computed from

$$\sigma_m = \frac{1}{2\pi} \int \int (1-\cos\chi)\, \frac{I(\chi,\phi)}{\Gamma}\, d\Omega\, d\phi, \tag{6}$$

where $I(\chi,\phi)$ is the number of MC particles scattered by angle $\chi$ into solid angle $d\Omega$ for starting azimuth angle $\phi$ per unit time, and $\Gamma$ is the flux of MC particles [see Fig. 3(b)]. Separate statistics were gathered for MC particles which were scattered and collected by the agglomerate.

It is important to note that the momentum transfer cross sections obtained here using a drift-diffusion formulation for the ions in the plasma model may differ from those obtained using a plasma model in which ion inertia and orbital motion

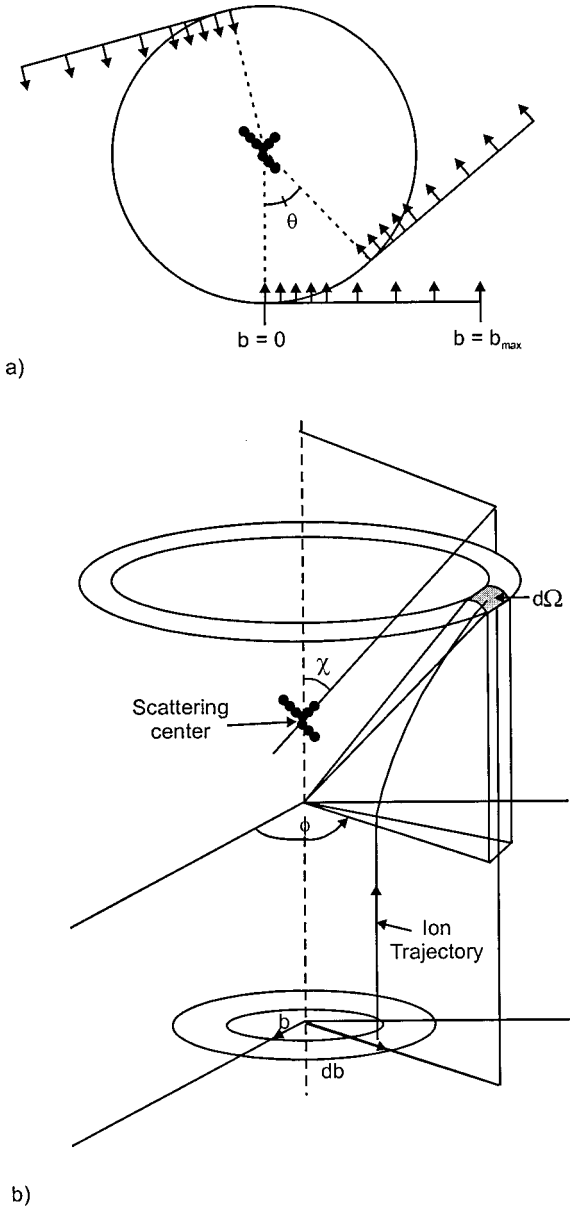


FIG. 3. Schematic of the particle launch sequence for the momentum transfer calculation. (a) For each angle of incidence, $\theta$, the launch locations are given by a predetermined set of impact parameters, $b$, for which the spacing is small near zero to resolve the shape of the agglomerate and gets progressively larger at larger impact parameters. (b) Schematic of the momentum transfer cross section calculation described by Eq. (6).

are accounted for. This difference results from the shielding length most likely being overestimated in this model, which then produces ion momentum transfer cross sections which are also larger. One should, however, keep in mind that the parameter of interest is the ratio of the shielding length to the characteristic dimension of the agglomerate. The systematic trends we discuss for the ion momentum transfer cross sections and other properties should apply to conditions for the same value of this parameter where ion inertia is accounted for.

## III. PROPERTIES OF AGGLOMERATES WITH COMPLEX SHAPES

The plasma conditions used in this study are argon gas at 200 mTorr having an ion density far from the agglomerate of

$3\times10^{10}$ cm$^{-3}$, an ion temperature of 500 K, and an electron temperature of 1.0 eV. Initially, the ion and electron and ion densities are uniform throughout the computational domain except for near the agglomerate, where they are linearly varied from zero at the particle surface to their maximum at a distance of the linearized Debye length. The initial agglomerate surface and bulk charge density is set to zero. The primary dust particle radius is 5 $\mu$m, a size chosen so that the computed shielding length would be commensurate with the size of some of the larger agglomerates investigated. For these cases, the primary dust particles are perfect dielectrics, have a permittivity of $20\cdot\epsilon_0$ and the surface and bulk conductivities are set to zero. Agglomerates are constructed by randomly ''assembling'' primary particles with separation slightly smaller than the sum of their individual radii, thereby giving, for example, a chain agglomerate with a somewhat ''compressed'' appearance.

The electric potential near a single primary particle is shown in Fig. 4(a). The surface charge density is shown in Fig 5(a). The potential on the particle is symmetric and equal to 6.57 V, commensurate with the floating potential for the selected plasma conditions. The shielding distance is 37 $\mu$m (defined as the $e$-folding distance for the potential) whereas the electron Debye length is 43 $\mu$m and the linearized debeye length is 12 $\mu$m. The charge density on the surface of the particle is also symmetric. The peak charge density for the particle in Fig. 5(a) is $9.56\times10^{12}$ $q$ cm$^{-3}$. This value corresponds to a surface charge density of $4.5\times10^{9}$ $q$ cm$^{-2}$, which is the equivalent of approximately 15 000 unit charges on an equivalent sphere.

The electric potential and surface charge for agglomerates having 4, 8 and 16 primary particles appear in Figs. 4 and 5, respectively. The maximum potential increases slightly with increasing size of the agglomerate (6.74, 6.76, 6.80 V), but does not deviate far from the floating potential of the single sphere case. As the agglomerate increases in size to be commensurate with the shielding length, the electric potential is perturbed to conform to the shape of the particle, vestiges of which extend to the edge of the sheath. In the case of the 16 particle agglomerate, the largest lateral dimension is 84 $\mu$m, whereas the shielding distance is 73 $\mu$m, which allows the electrical potential to be fairly conformal.

As the agglomerate increases in size, and takes on a more dendritic shape having a lower fractal dimension, the distribution of charge becomes less uniform. For example, with the 16 particle agglomerate, the outer ''convex'' surfaces of the particle have significantly more charge than the inner ''concave'' surfaces. Protruding apexes collect the greatest amount of charge. Although this is a steady state configuration, the charge distribution is not a unique solution and depends, to some degree, on the initial conditions. For example, by starting with a uniform and large plasma density, the apexes of the agglomerate, having the largest solid viewing angle to the plasma, collect the most flux and charge the fastest. Since the charging time scales with the plasma density, the apex rapidly achieves a steady state surface charge. The inner surfaces have a small solid viewing angle to the plasma, and so collect a proportionally smaller amount

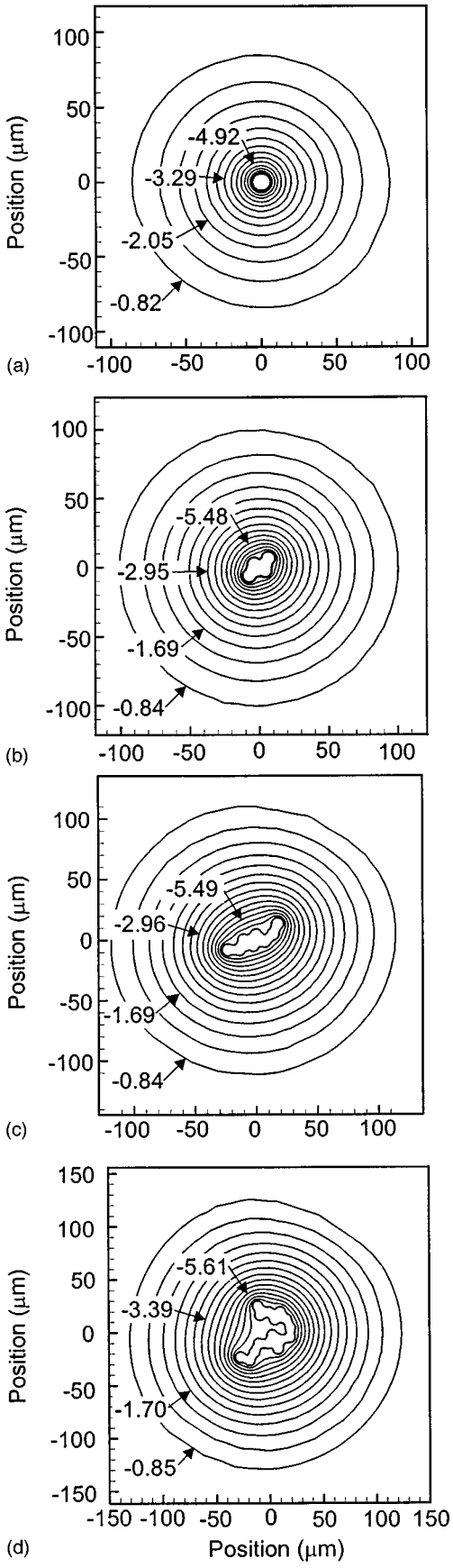


FIG. 4. Electrostatic potentials around agglomerates: (a) single particle. (b) 4 particle agglomerate, (c) 8-particle agglomerate, and (d) 16 particle agglomerate. As the agglomerate size approaches the plasma shielding length, the potential becomes more conformal around the agglomerate.

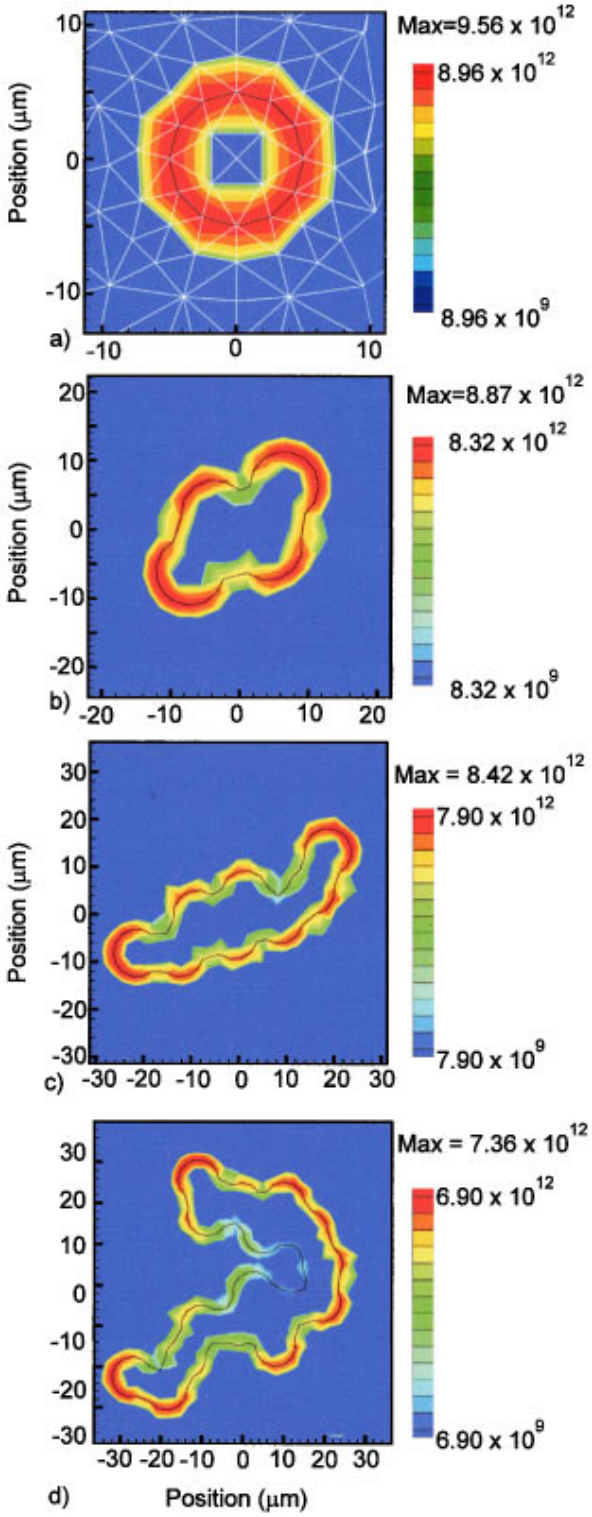


FIG. 5. Charge density on agglomerates. (a) Single particle, (b) 4 particle agglomerate, (c) 8 particle agglomerate, and (d) 16 particle agglomerate. The charge is plotted over a dynamic range of three decades in units of $Q/q$ $cm^{-3}$, where $q$ is the electron charge.

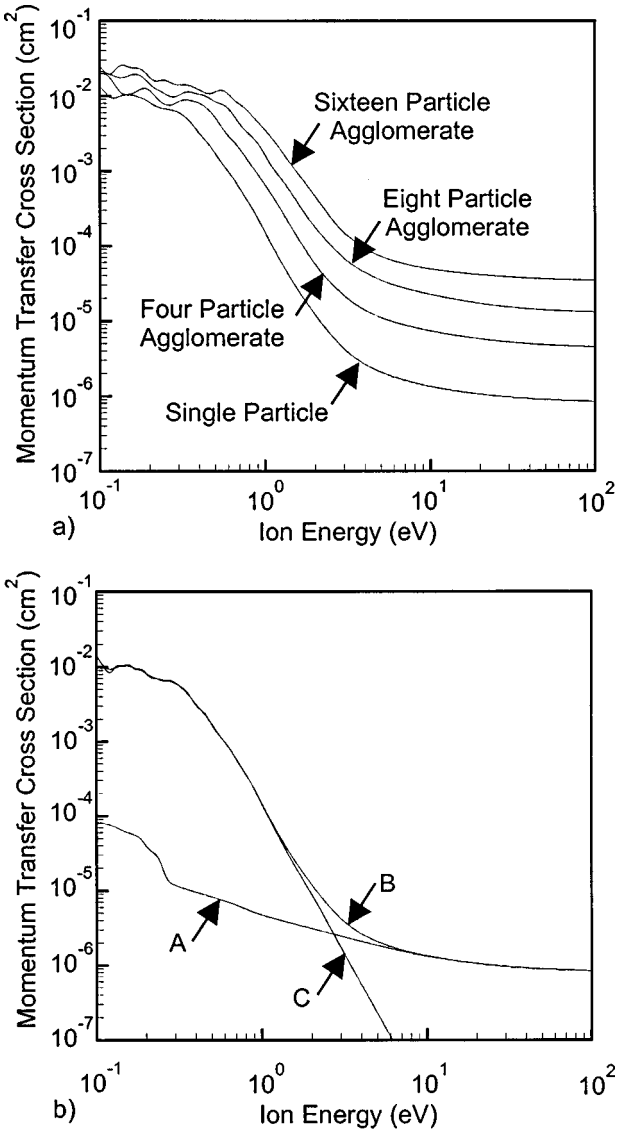


FIG. 6. Ion-drag momentum transfer cross sections. (a) Cross sections as a function of ion energy for 1, 4, 8 and 16 particle agglomerates. These cross sections correspond to the conditions shown in Figs. 4 and 5. (b) Cross section as a function of ion energy for a single sphere. The total cross section is labeled 'B', the contribution from ions that collide with the particle are labeled 'A', while the ion orbital contribution to the cross section is labeled 'C'. As the number of monomer particles in the agglomerate increases, the asymptotic high energy limit for the cross section increases, and the exponential scaling factor (or slope) for the falloff regime decreases.

of flux which is further diminished by losses to surfaces. To first order, however, the surface charge density depends on the ratio of electron to ion temperatures, and not the magnitude of the fluxes. Therefore, one might expect the inner concave surfaces also to eventually charge to same potential as the apexes. The charged apexes, however, act as ''gatekeepers,'' having a potential which repels electron flux from entering the crannies, thereby reducing the charging required of their surfaces to balance electron and ion fluxes.

Ion-drag momentum transfer cross sections as a function of ion energy are shown in Fig. 6(a) for the 1, 4, 8 and 16 particle agglomerates. The momentum transfer cross section is the sum of ions undergoing orbital or elastic momentum exchange, and those ions which collide with the agglomerate. An illustration of these two contributions is shown in Fig. 6(b). The cross sections have a low energy component due largely to the orbital motion of the ions at large impact parameter. This is followed by a falloff regime and an asymptotic high energy component. The high energy compo-

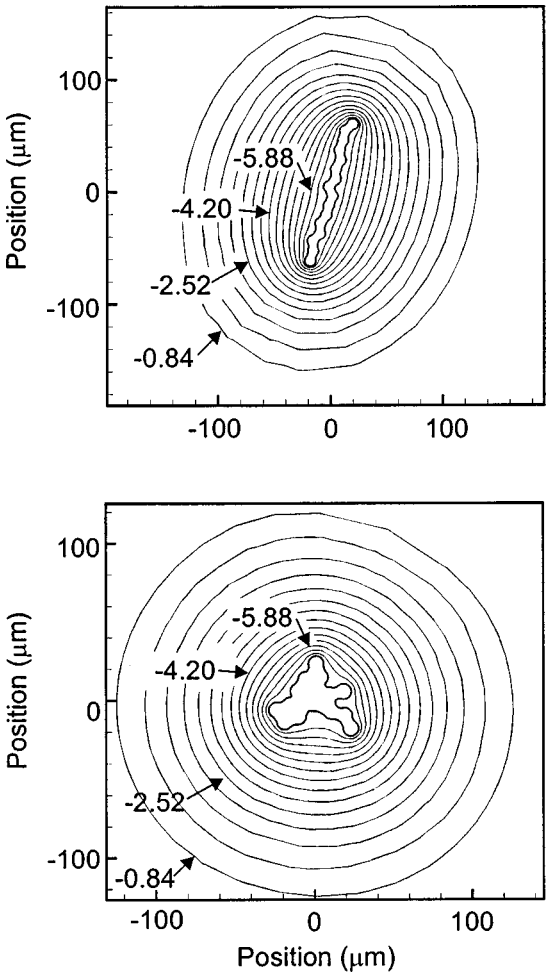


FIG. 7. Electrostatic potential around 16 particle agglomerates having different shapes. (a) Linear agglomerate and (b) compact agglomerate. The contour labels are in volts.

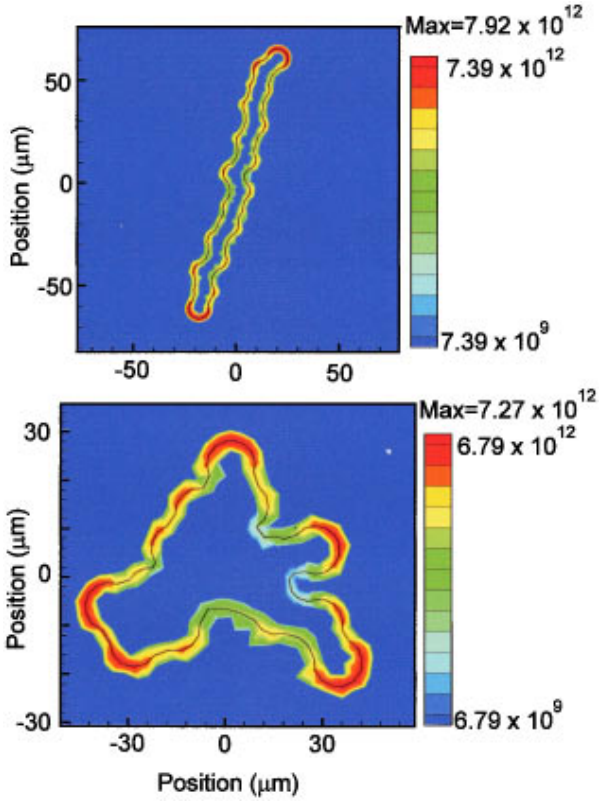


FIG. 8. Surface charge on 16 particle agglomerates having different shapes. (a) linear agglomerate and (b) compact agglomerate. The charge is plotted over a dynamic range of three decades in units of $Q/q$ cm$^{-3}$, where $q$ is the electron charge.

nent is due to ions collected by the agglomerate and scales with its ''angle averaged'' cross sectional area. Since, to first order, the ion momentum transfer cross section in the falloff regime can be approximated by a Coulomb-Coulomb interaction, the energy dependence should scale as $\epsilon^{-x}$ regardless of the magnitude of the size of the agglomerate. The exponential dependence in the falloff regime, however, varies as a function of size of the agglomerate. In these cases, the exponent is 2.76, 2.39, 2.28, and 2.29 for the 1, 4, 8 and 16 particle agglomerates. The differing exponents imply there is a shape scaling to the ion-drag cross section which is due, in part, to the fact that $L/\lambda$ (agglomerate scale length/shielding distance) is of order unity.

The cited scaling in ion momentum cross section may also reflect a change in the fractal dimension (or dendritic nature) of the agglomerate. To investigate this scaling, we constructed 16 particle agglomerates having different morphologies. The resulting electric potentials and charge densities for a nearly linear agglomerate and a compact agglomerate are shown in Figs. 7 and 8. We see that the potential contours closely follow the morphology of each agglomerate, and that the minimum potentials are approximately the same for each case ($-6.72$ V). The surface charge distribution shows the familiar maxima at convex apexes and minima in concave valleys. The corresponding ion-drag cross sections are shown in Fig. 9. In comparing the two cross sections the compact agglomerate, the linear agglomerate has a larger angle averaged cross sectional area, and therefore the spatial extent of its potential well is also larger. As a result, the high energy limits for the cross section for the two agglomerates are different. The linear agglomerate asymptotically approaches $8.1\times10^{-5}$ cm$^2$ and the compact case $2.2\times10^{-5}$ cm$^2$. In the falloff regime, the exponent for the energy dependence of the cross section of the linear agglomerate is 2.18 and for the compact agglomerate is 2.49. These values bracket the exponent for the energy dependence of the cross section for the moderately compact 16 particle agglomerate in Fig. 6 whose value was 2.29. More compact agglomerates having larger fractal dimensions appear to have both smaller ion-drag cross sections and a more rapid falloff at higher ion energies. This morphology dependence becomes more acute with increasing agglomerate size since the potential contours are more conformal around the larger agglomerates. The dynamic range of spatial scales also increases as the degree of agglomeration increases, thereby enabling a greater degree of morphology dependence.

Recall that these ion momentum transfer cross sections were obtained by averaging ion trajectories which are isotropically incident onto the agglomerate. The cross sections are therefore most applicable to agglomerates in the bulk plasma or where there is no preferred orientation of the agglomerates with respect to the net direction of the ion flux. There cer-

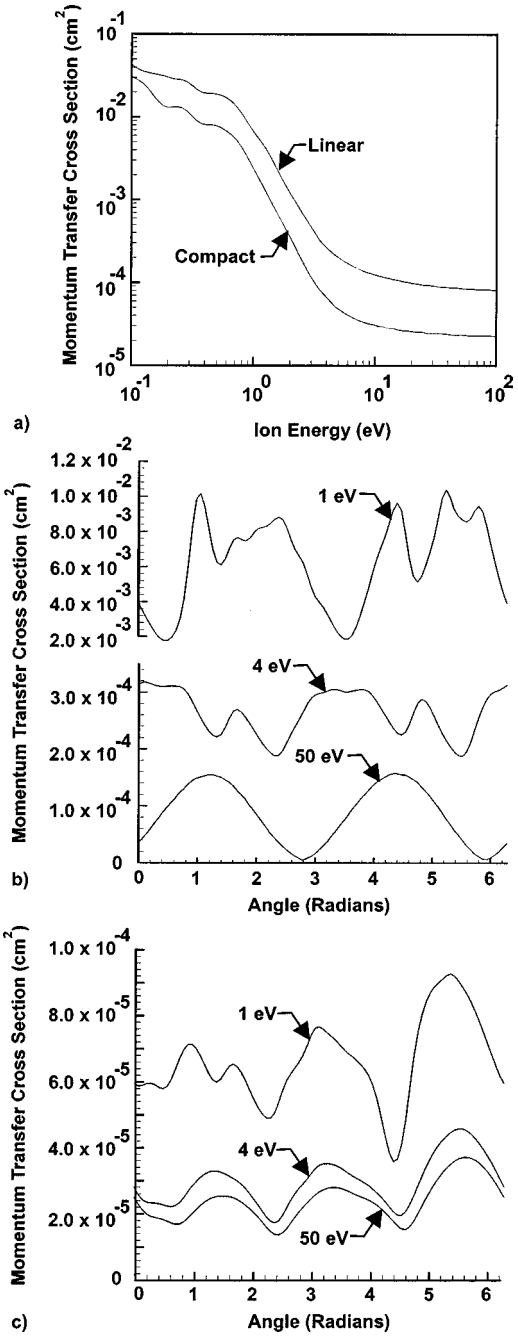


FIG. 9. Ion-drag momentum transfer cross sections for 16 particle agglomerates. (a) Cross sections for the linear and compact shapes shown in Figs. 7 and 8. (b) Cross sections for the linear agglomerate as a function of the angle of incidence of the ion for energies of 1, 4 and 50 eV. (c) Cross sections for the compact agglomerate as a function of the angle of incidence of the ion for energies of 1, 4 and 50 eV.

tainly is a dependence of the ion momentum transfer cross section on the angle of incidence of the ion, and particularly so for agglomerates having a low fractal dimension. For example, ion momentum transfer cross sections as a function of angle of incidence are shown in Figs. 9(b) and 9(c) for the linear and compact agglomerates, respectively. Cross sections are shown for fixed ion energies of 1, 4 and 50 eV. For both the linear and compact cases, the cross sections having the least structure are for the highest ion energy, 50 eV. This energy corresponds to the high energy asymptotic regime in which the cross section approaches the projected cross sectional area of the agglomerate. For the linear agglomerate, the cross section is smallest for the agglomerate orientations which are parallel to the initial ion velocity and are largest for orientations which are perpendicular. This angular dependence is approximately maintained as the ion energy is decreased, however the angular dependence has more structure. At lower energies, the ion trajectories are more influenced by the shielding electric fields which conformally surround the particle. Small undulations in these fields, resulting from the fact that the agglomerate is not a strictly linear object, produce extrema in the cross sections. Ion momentum cross sections for the compact agglomerate show similar, but not as severe, angular dependence. For example, the cross section for the 50 eV ion is modulated as a function of angle, however the depth of the modulation is smaller than for the linear agglomerate since the projection of the compact agglomerate is more uniform as a function of angle.

## IV. CONCLUDING REMARKS

A plasma model using an unstructured mesh has been developed to investigate plasma transport and charging of dust particle agglomerates having complex shapes in partially ionized plasmas. We found that the surface charge on multi-particle agglomerates tended to be nonuniform, and that the nonuniformity depended primarily on the morphology of the particle. Convex apexes of dielectric agglomerates tended to collect more charge than concave valleys, and act as ''sentinels'' which shield further charging of those valleys. Morphology therefore determined the surface charge distribution by both geometrical and electrostatic charging effects.

To investigate how the shape of a complex agglomerate affects its transport in a plasma, ion-drag momentum transfer cross sections were calculated using a Monte Carlo simulation using the electric potential distributions obtained from the plasma simulation. The calculated cross sections were significantly different as a function of both the overall size of the agglomerate and the fractal dimension. Agglomerates consisting of larger numbers of constituent monomer particles tended to have larger cross sections for high kinetic energy and smaller exponents for the falloff regime. Agglomerates having the same number of constituent monomer particles but differing levels of fractal dimension also displayed differences in these same characteristics. An agglomerate of high fractal dimension (compact) typically had a smaller high energy cross section and a larger exponential scaling factor than an agglomerate of low fractal dimension (linear) having the same number of constituent monomer particles. This effect is more pronounced for large agglomerates in which the spatial scale exceeds the electrostatic screening length, and the potential contours are forced to more closely conform to the shape of the particle. These results imply that ion-drag forces are larger on low fractal dimension agglomerates (i.e., chainlike agglomerates) and so particle contamination of wafers by these agglomerates is more likely. The ion-drag cross sections are functions of the angle of incidence of the ion. Plasma conditions which result

in there being a preferred orientation of the incident ion trajectories with respect to the agglomerate will produce cross sections which are functions of that orientation.

## ACKNOWLEDGMENTS

This work was supported by the Semiconductor Research Corporation, National Science Foundation (ECS 94-04133, CTS 94-12565), Defense Advanced Research Projects Administration and the University of Wisconsin ERC for Plasma Aided Manufacturing.

[1] A collection of papers addressing particle transport in plasma processing reactors appears in a special issue of Plasma Sources Sci. Technol. **3**, 239 (1994), and of the J. Vac. Sci. Techol. A **14**, 489 (1996).
[2] S. J. Choi and M. J. Kushner, IEEE Trans. Plasma Sci. **22**, 138 (1994).
[3] F. Y. Huang and M. J. Kushner, J. Appl. Phys. **81**, 5960 (1997).
[4] D. B. Graves, J. E. Daugherty, M. D. Kilgore, and R. K. Porteous, Plasma Sources Sci. Technol. **3**, 433 (1994).
[5] CFD Research Corporation, Huntsville, AL, http://www.cfdrc.com
[6] K. M. Kramer and W. N. G. Hitchon, Comput. Phys. Commun. **85**, 167 (1995).
[7] S. Selberherr, *Analysis and Simulation of Semiconductor Devices* (Springer, Wien, 1984).
[8] D. L. Scharfetter and H. K. Gummel, IEEE Trans. Electron Devices **16**, 64 (1969).